Interactions Between Light-Induced Currents, Voltage-Gated Currents, and Input Signal Properties in Drosophila Photoreceptors

Jeremy E. Niven, Mikko Vähäsöyrinki, Mikko Juusola and Andrew S. French

J Neurophysiol 91:2696-2706, 2004. First published Jan 28, 2004; doi:10.1152/jn.01163.2003

J Neurophysiol 91: 2696–2706, 2004.
First published January 28, 2004; 10.1152/jn.01163.2003.

Interactions Between Light-Induced Currents, Voltage-Gated Currents, and Input Signal Properties in *Drosophila* Photoreceptors

Jeremy E. Niven,[1] Mikko Vähäsöyrinki,[2] Mikko Juusola,[1] and Andrew S. French[3]

[1]*Physiological Laboratory, University of Cambridge, Cambridge CB2 1TN, United Kingdom;* [2]*Division of Biophysics, Department of Physical Sciences, University of Oulu, Oulu, FIN-90014, Finland; and* [3]*Department of Physiology and Biophysics, Dalhousie University, Halifax, Nova Scotia B3H 1X5, Canada*

Submitted 4 December 2003; accepted in final form 21 January 2004

Niven, Jeremy E., Mikko Vähäsöyrinki, Mikko Juusola, and Andrew S. French. Interactions between light-induced currents, voltage-gated currents, and input signal properties in *Drosophila* photoreceptors. *J Neurophysiol* 91: 2696–2706, 2004. First published January 28, 2004; 10.1152/jn.01163.2003. Voltage-gated K^+ channels are important in neuronal signaling, but little is known of their interactions with receptor currents or their behavior during natural stimulation. We used nonparametric and parametric nonlinear modeling of experimental responses, combined with Hodgkin–Huxley style simulation, to examine the roles of K^+ channels in forming the responses of wild-type (WT) and *Shaker* mutant (Sh^{14}) *Drosophila* photoreceptors to naturalistic stimulus sequences. Naturalistic stimuli gave results different from those of similar experiments with white noise stimuli. Sh^{14} responses were larger and faster than WT. Simulation indicated that, in addition to eliminating the *Shaker* current, the mutation changed the current flowing through light-dependent channels [light-induced current (LIC)] and increased the delayed rectifier current. Part of the change in LIC could be attributed to direct feedback from the voltage-sensitive ion channels to the light-sensitive channels by the membrane potential. However, we argue that other changes occur in the light detecting machinery of Sh^{14} mutants, possibly during photoreceptor development.

INTRODUCTION

Sensory systems are thought to be tuned to the statistical properties of their natural stimuli through evolutionary and/or developmental processes (e.g., Katz and Shatz 1996; Weckström and Laughlin 1995). Therefore understanding how specific components function within these sensory systems should benefit from using stimuli with appropriate dynamic properties. Natural visual inputs often contain strong temporal and spatial correlations, as well as large intensity fluctuations (Burton and Moorhead 1981; Field 1987; Ruderman and Bialek 1994; Srinivasan et al. 1982; Tolhurst et al. 1992) that may cause sparse, brief, intense firing events (Reinagel 2001; Vinje and Gallant 2000, 2002), and activate components such as ion channels that strongly influence neural coding. However, sensory systems are usually investigated using simpler, easily characterized stimuli, such as pulses, steps, or white noise (e.g., French 1980; Juusola and Hardie 2001; Juusola et al. 1994; Laughlin and Hardie 1978; Zettler 1969). These experiments have yielded considerable insights into sensory systems but are unlikely to predict responses to natural stimuli.

Linear systems have the property of superposition, allowing measurements from a restricted range of stimuli to predict the response to any stimulus. This is not true for nonlinear systems, including many physiological systems (Marmarelis and Marmarelis 1978). Responses of neural systems or components to one set of stimuli may not predict their responses to other inputs (Burton and Laughlin 2003; Chacron et al. 2003; Juusola and de Polavieja 2003; Lewen et al. 2001; Niven and Burrows 2003; Rieke et al. 1995; Rinberg and Davidowitz 2000; van Hateren 1997; Vickers et al. 2001). For example, responses to white noise stimulation of lateral geniculate nucleus neurons did not predict responses to naturalistic stimuli (Dan et al. 1996).

Drosophila photoreceptors provide an important system for measuring the contributions of individual neural components, such as ion channels, to overall behavior in vivo (Hardie 1991a; Hardie et al. 1991; Juusola and Hardie 2001; Niven et al. 2003a). Their membranes contain at least 3 groups of voltage-gated potassium channels, including *Shaker* and delayed rectifier (Hardie 1991; Hardie et al. 1991). We previously examined the role of *Shaker* channels on information processing in *Drosophila* photoreceptors using white noise stimulation (Juusola et al. 2003; Niven et al. 2003a,b) and suggested that they could significantly modulate responses to natural stimuli. To determine the contributions of light-dependent ion channels and voltage-gated K^+ channels to photoreceptor responses during naturalistic stimuli, we have now recorded intracellularly from wild-type (WT) and Sh^{14} *Drosophila* photoreceptors while presenting light modulated by a natural time series of intensities (NTSIs) (van Hateren 1997; van Hateren and Snippe 2001). Sh^{14} flies have a missense mutation in the *Shaker* potassium channel core region, which generates nonfunctional channels (Kaplan and Trout 1961; Salkoff and Wyman 1981). Comparison of WT and Sh^{14} photoreceptor responses suggested that *Shaker* channels increase the response spread across the available voltage range during naturalistic stimuli. To quantify these effects, photoreceptor responses were modeled by both Volterra series and nonlinear–linear–nonlinear (NLN) cascades. These revealed that Sh^{14} photoreceptor responses to naturalistic stimuli were significantly different from their responses to white noise stimuli. A Hodgkin–Huxley type model was used to separate the contributions of the current through light-dependent channels [light-induced current (LIC)] and the current through voltage-activated ion channels to the total voltage response. This model showed that differences in the response nonlinearities of both WT and Sh^{14} photoreceptors

Address for reprint requests and other correspondence: A. S. French, Department of Physiology and Biophysics, Dalhousie University, Halifax, Nova Scotia B3H 1X5, Canada (E-mail: andrew.french@dal.ca).

The costs of publication of this article were defrayed in part by the payment of page charges. The article must therefore be hereby marked "*advertisement*" in accordance with 18 U.S.C. Section 1734 solely to indicate this fact.

were primarily attributed to changes in LIC, suggesting that feedback from the effects of voltage-gated ion channels to light transduction may be important for tuning photoreceptor responses during development.

METHODS

Fly stocks

The wild-type strain was red-eyed *Drosophila melanogaster* Oregon Red. Mutant animals with Sh^{14}, a missense mutation in the core region resulting in nonfunctional *Shaker* channels (Kaplan and Trout 1961), were also red-eyed flies. Both strains of flies were raised at 19°C in darkness.

Recording and stimulation

Recording, stimulation, and data acquisition were previously described (Juusola and de Polavieja 2003; Juusola and Hardie 2001). Photoreceptors were stimulated by a high-intensity green light-emitting diode (LED) with peak wavelength of 525 nm (Marl Optosource). Light intensity was derived from a published naturalistic stimulus time series obtained from a light detector moving through a natural environment (van Hateren 1997; van Hateren and Snippe 2001). The light stimulus was presented at a rate of 1 kHz and all the light intensity measurements were converted to dimensionless contrast units. Light intensity and photoreceptor membrane potential were sampled at 1-ms intervals during repeated presentations of naturalistic light sequences of 18-s duration. Photoreceptors were only used if their membrane potential was more negative than −55 mV and they had at least a 45-mV saturating impulse response in dark-adapted conditions.

The light source gave an approximately monochromatic, small-field stimulus, whose angle of 5.4° covered more than one ommatidium, so that stimuli delivered to different units were not statistically independent. LEDs also have compressive nonlinearities that caused the actual output to differ from the collected NTSIs. The light stimulus was presented at a rate of 1 kHz, instead of the original recording rate of 1.25 kHz, which decreased the frequency bandwidth of the stimulus. This allowed direct comparison with our previous data obtained by white noise stimulation (Juusola et al. 2003), and was justified by the relatively slow flying speeds of *Drosophila* (David 1978; Fry et al. 2003). Although these differences from natural outdoor spatial and chromatic light patterns must be noted, they should not affect the general validity of the analysis.

Nonlinear system identification

Identification was based on estimating the kernels of a Volterra series, K_0, $K_1(u)$, $K_2(u, v)$, $\cdots$, where u, v, $\cdots$ are time lags (French and Marmarelis 1999) with light intensity as the input $x(t)$, as a function of time t, and receptor potential as the output $y(t)$. Several methods have been developed for kernel estimation. Earlier methods relied on stimulating the unknown system with Gaussian white noise, but more recent methods avoid this requirement (French and Marmarelis 1999). We used a completely general approach based on a parallel cascade method (Juusola et al. 2003; Korenberg 1991), but having the linear filters of the cascades formed from Gaussian-distributed random numbers (French et al. 2001; Juusola et al. 2003). This method makes no initial assumptions about the forms of the kernels or the nature of the input or output signals and it can be applied to systems containing a relatively high order of nonlinearities. However, it is not necessary to construct all of the higher-order kernels.

Responses to 12 presentations of an 18-s sequence of naturalistic stimulus light contrast were concatenated, and the original sampling resolution of 1 ms was reduced to 2 ms by combining adjacent points to give records of 108,000 data pairs (light intensity in contrast units and receptor potential in mV). This was done both to reduce the fitting tasks and to accommodate the relative lack of high-frequency components in the NTSI. For each record, the first 50,000 data pairs were discarded to avoid any effects resulting from the onset of light stimulation. The following 40,000 data pairs were analyzed as the input and output of the unknown nonlinear dynamic system.

After kernel estimation, percentage mean square error (MSE) values (French and Marmarelis 1999) were calculated for the zero- and first-order kernels alone and for the combined, zero-, first-, second-, and third-order kernels from

$$\mathrm{MSE} = 100\,\frac{\overline{[y(t) - y_s(t)]^2}}{\overline{y^2(t)} - \overline{[y(t)]^2}} \qquad (1)$$

where $y_s(t)$ is the Volterra series output and the bars indicate time averages.

The kernel estimates were then used to predict the output of the nonlinear system to the input signal of the remaining 10,000 data pairs of each record. Therefore all predictions were based on recorded data that had not been used for system identification.

Simulation: NLN model

Nonlinear responses in *Drosophila* photoreceptors were simulated by an NLN (nonlinear static–linear dynamic–nonlinear static) cascade model (French et al. 1993). The two nonlinear components were polynomial functions and the linear component was the Wong and Knight photoreceptor model (Wong et al. 1980)

$$g(t) = \frac{1}{n!\tau}\left(\frac{t}{\tau}\right)^n \mathrm{e}^{-t/\tau} \qquad (2)$$

where n and τ are parameters to be fitted. To remove redundant parameters, only one constant term was included in the model, as an offset in the output of the linear component. Similarly, the first nonlinear component had a fixed first-order coefficient of unity. The numbers of unknown parameters were therefore: $N_1 - 1$ (first polynomial) + 3 (Wong and Knight model plus offset) + N_2 (second polynomial). The NLN cascade model was fitted to the first 9,000 data pairs (corresponding to one complete cycle through the naturalistic stimulus sequence) used for the kernel analysis. Fitting was performed by simulated annealing (Press et al. 1990). The fitting algorithms always converged satisfactorily. MSE values were again calculated using *Eq. 1*.

Simulation: Hodgkin–Huxley photoreceptor model

A Hodgkin–Huxley type photoreceptor model was developed using MATLAB software (MathWorks, Natick, MA). Derivation and validation of the model were described previously (Niven et al. 2003a; supplementary material). The model included *Shaker* and delayed rectifier potassium conductances, in addition to potassium and chloride leak conductances. The voltage-dependent parameters (including time constants and steady-state functions for activation and inactivation) for the *Shaker* and delayed rectifier conductances were obtained from published data (Hardie 1991; Hevers and Hardie 1995; Niven et al. 2003a). Other photoreceptor membrane properties (i.e., the maximum values of the active conductances, resting potential, leak conductances, and membrane capacitance) were estimated from in vivo recordings. The voltage-dependent properties of the ion channels, the reversal potentials for each ion, and the membrane area were kept fixed in all simulations. Potassium and chloride leak conductances in the model were adjusted for each individual photoreceptor until the experimental resting potential and steady-state resistance were obtained. Maximum conductances for the *Shaker* and delayed rectifier channels were also adjusted to fit the experimental data.

The model allowed us to predict the current flowing through light-dependent channels (LIC) attributed to NTSI. Although the voltage-dependent properties of *Shaker* and delayed rectifier conductances were characterized in darkness, these properties were assumed to be insensitive to light. This was justified both by comparison of simulated voltage responses to current stimuli with experimental data (data not shown), and by experimental results from *Calliphora* photoreceptors (Weckström et al. 1991). The absorption of a single photon happens in all-or-none fashion, causing influx of calcium and sodium ions to a microvillus. The small microvillar volume leads to rapid changes in ionic concentrations, and a reversal potential of +10 mV for this light-induced conductance (Oberwinkler and Stavenga 2000; Reuss et al. 1997). During natural stimuli the photon flux must activate numerous microvilli, causing dynamic reversal potential fluctuations in each microvillus as it receives photons. These fluctuations were assumed to be independent and were modeled as a single average light-induced conductance input to the light-insensitive membrane. This conductance was used to drive the Hodgkin–Huxley model and its values were iterated at each sample point until the experimental voltage response was reproduced. From each simulation the individual model conductances, including *Shaker*, delayed rectifier and light-induced conductance, were used to calculate the corresponding currents I_i from the electrical driving force of the individual ions and their conductances g_i, using Ohm's law

$$I_i = g_i(V_m - E_i) \quad (3)$$

where V_m is the membrane potential and E_i represents the reversal potentials of the ions.

Predicted LICs produced voltage responses that closely matched experimental data, except during total darkness (data not shown). This was also true for the nonlinear kernel and NLN models (Fig. 2). Experimental data contained clear afterhyperpolarizations in the WT and the mutant responses, as well as small depolarizations preceding afterhyperpolarizations in the mutant response (Fig. 2). These are caused by the Na^+/K^+ pump and the $3Na^+/Ca^{2+}$ exchanger currents, respectively (Gerster 1997; Gerster et al. 1997; Oberwinkler and Stavenga 2000). Estimated amplitudes of these currents are about 10 times smaller than the other currents in the model (Fig. 5), indicating that they would not affect our analysis. As a further test, an NLN model was derived from the simulated voltage response of the Hodgkin–Huxley model. The components in this NLN model were identical to those derived from experimental data, confirming that the smaller currents do not cause significant errors.

Data analysis and graphical presentations were performed by custom-written software using the C++ programming language and PC-compatible desktop computers.

RESULTS

Responses of WT and Sh^{14} photoreceptors to naturalistic stimuli

We recorded intracellularly from WT and mutant (Sh^{14}) photoreceptors in vivo while presenting NTSI stimuli. The naturalistic stimuli contained periods of both very low and high light intensity that were reflected in the voltage responses of both the WT and mutant photoreceptors (Fig. 1*A*). Although the structure of both WT and Sh^{14} photoreceptor responses resembled the gross structure of the naturalistic light stimulus (Fig. 1*A*), examination of the fine structure of the responses revealed clear differences between the 2 photoreceptor types (Fig. 1*B*). These differences were particularly clear during sequences of rapid transients in which WT photoreceptors closely followed the light

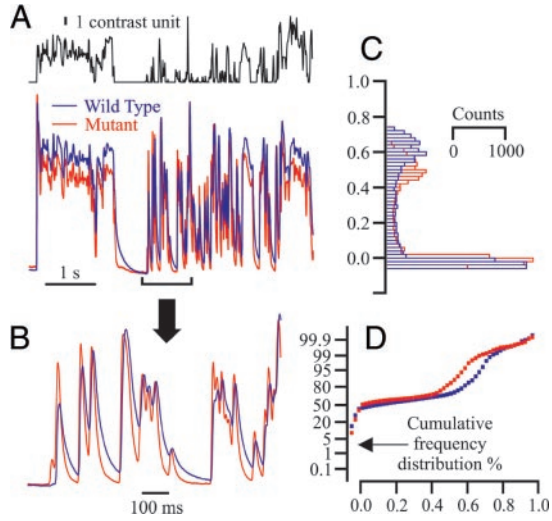

FIG. 1. Wild-type (WT) and Sh^{14} mutant *Drosophila* photoreceptors responded differently to the same naturalistic time series light stimulation. *A*: naturalistic stimulus (*top*) and normalized averaged responses of WT and mutant cells. *B*: portion of the same 2 traces using an expanded time scale. *C*: *frequency histograms* of complete response records. *D*: cumulative frequency distributions of the histograms, illustrating the differences in the responses of the 2 groups of photoreceptors. Note that the large histogram peaks, near zero in this and other figures, are partly attributed to the lack of very dim output from the LED source, and negative values represent responses that are hyperpolarized beyond the resting potential.

stimulus but Sh^{14} photoreceptors were unable to do so. For example, in Fig. 1*B* light intensity fluctuations of increasing intensity were encoded by increasing responses in the WT photoreceptor but the Sh^{14} responses approached plateau depolarizations at lower stimulus levels, compressing their responses to bright inputs. Mutant photoreceptors produced large, fast voltage responses to large light intensity increases after dim periods, which were reduced in WT photoreceptors (Fig. 1*B*). During sustained periods of bright light Sh^{14} receptors produced smaller responses than WT (Fig. 1*A*). Additionally, Sh^{14} voltage responses repolarized more rapidly than WT voltage responses (Fig. 1*A*). Differences in the voltage responses over the entire stimulus sequences are shown in the *response histograms* (Fig. 1*C*), and the cumulative frequency distributions of these histograms (Fig. 1*D*), which show that the voltage response of WT photoreceptors was spread over a greater voltage range than the mutant.

Characterization of the differences between WT and Sh^{14} photoreceptors

Measures commonly used to characterize graded neuronal responses, such as those of a photoreceptor, to Gaussian white noise stimuli cannot be used to characterize responses to natural stimuli because both stimulus and response are non-Gaussian. Therefore we used Volterra kernel series and NLN models of WT and Sh^{14} photoreceptor responses to NTSI sequences to characterize the effects of ion channels on natural stimulus coding (Figs. 2–4).

Responses of WT and Sh^{14} mutant photoreceptors to the same NTSI stimulation, together with predictions obtained from first-, second- and third-order Volterra kernel series (labels K_1, K_2, K_3, respectively) and NLN models are shown in Fig. 2. Mean square error (MSE, *Eq. 1*) data for all the

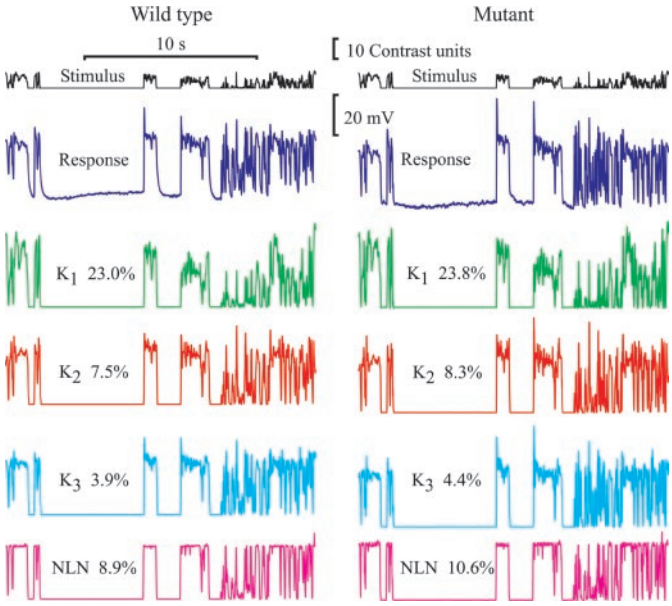

FIG. 2. Model predictions of *Drosophila* photoreceptor responses to naturalistic time series stimuli. *Top 2 traces*: stimulus and experimental responses for WT (*left*) and Sh^{14} mutant (*right*) photoreceptors, respectively. Next 4 *pairs of traces* show (in descending order) model predictions from first-, second-, and third-order Volterra series (labeled K_1, K_2, K_3, respectively) and from the nonlinear static–linear dynamic–nonlinear static (NLN) models. Numerical values on the traces are average mean square error values from 5 different experiments (Table 1).

experiments were consistent for all the experiments ($n = 5$ for each of the WT and Sh^{14} mutant flies), and values for WT and mutant flies were similar under all conditions (Fig. 2, Table 1). Linear models gave relatively large errors, approximately 25%, but second-order models reduced the error to approximately 8% and third-order models to only approximately 4%, indicating strongly nonlinear behavior in the photoreceptors. The main difference between these models was the degree to which they captured the time course of adaptation in the photoreceptor voltage responses (Fig. 2). The NLN model had MSE values of approximately 10%, similar to those of the second-order Volterra kernel models (Fig. 2, Table 1).

TABLE 1. *MSE values for Volterra kernel and NLN models of experimental data*

	Volterra Kernel Model			
Photoreceptor	K_1	$K_1 + K_2$	$K_1 + K_2 + K_3$	NLN Model
Wild type	22.2	6.5	3.0	7.81
	18.5	5.0	2.3	7.19
	25.9	9.0	4.6	11.35
	26.5	10.7	6.9	9.50
	21.9	6.2	2.9	9.09
Means	23.0	7.48	3.94	8.98
Sh^{14}	29.4	13.9	9.4	13.23
	24.5	7.6	3.2	10.21
	24.2	7.8	3.3	11.13
	21.2	6.3	3.1	10.45
	19.8	5.7	2.8	7.99
Means	23.82	8.26	4.36	10.60

All values are expressed as percentage. NLN, nonlinear static–linear dynamic–nonlinear static.

WT and Sh^{14} photoreceptor responses to naturalistic stimuli have novel kernel forms

First-order kernels, $K_1(u)$, derived from WT and Sh^{14} voltage responses to naturalistic stimuli had the same general form as flash responses in light-adapted *Drosophila* photoreceptors (Fig. 3*A*; Juusola and Hardie 2001). All of the first-order kernels had a delay of about 6 ms, but the kernels derived from Sh^{14} voltage responses consistently had faster time-to-peak (~3–4 ms) and narrower half-width than those from WT voltage responses (Fig. 3*A*). This feature corresponds with the larger and faster Sh^{14} voltage responses clearly visible in the voltage responses shown in Fig. 1, *A* and *B*.

We compared the kernel forms derived from voltage responses to naturalistic stimuli with those derived from Gaussian white noise stimuli (Juusola et al. 2003). Comparison of WT and Sh^{14} kernels from the 2 stimulus regimes revealed that the Sh^{14} kernel peaked later under white noise conditions. Indeed, WT and Sh^{14} kernels derived from white noise stimuli were indistinguishable (Fig. 3*B*). In addition to these changes in the timing and amplitude of the Sh^{14} kernels, those derived from naturalistic stimuli were less smooth than those obtained by white noise stimulation (Fig. 3, *A* and *B*; Juusola et al. 2003). One reason for this is that the selected NTSI stimulus had relatively small amplitude components at high frequencies, causing poor estimation of high frequencies and leading to

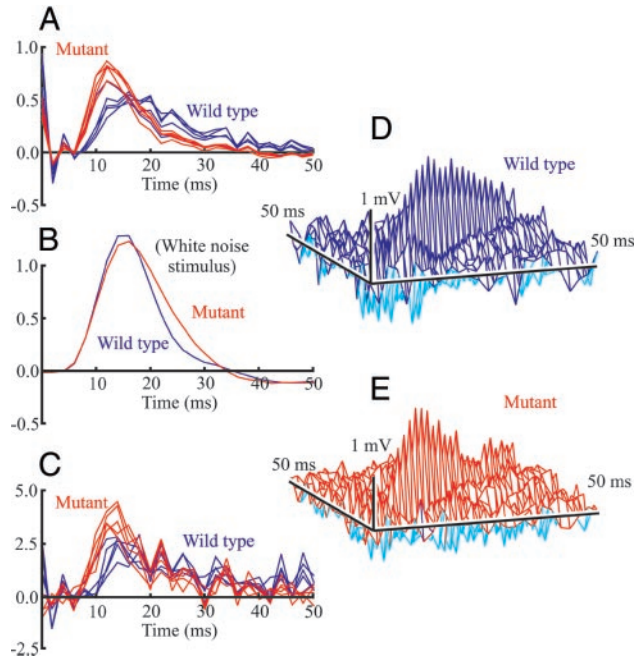

FIG. 3. Volterra kernels for phototransduction in *Drosophila* photoreceptors. *A*: kernels from 5 WT and 5 Sh^{14} mutant *Drosophila* photoreceptors obtained by fitting a first-order (linear) Volterra series. *B*: for comparison, kernels obtained by white noise stimulation (Juusola et al. 2003) are shown. *C*: first-order kernels obtained by fitting a third-order series. Increased amplitude in this bottom plot indicates that higher-order kernels contain components that attenuate the kernels measured by linear fitting. Mutant photoreceptors consistently gave larger and faster first-order kernels to natural time series of intensities (NTSI) stimulation. *D* and *E*: second-order kernels for phototransduction in WT and Sh^{14} mutant *Drosophila* photoreceptors, respectively, obtained by fitting a third-order Volterra series. Although the kernels are complex, both show strong diagonal components with similar time courses to the first-order kernels, characteristic of systems containing strong static nonlinearities feeding time-dependent linear filters. Mutant responses again peaked earlier than WT.

increased variance in the time domain kernel estimates. Another factor is the strongly nonlinear behavior of photoreceptors to NTSI, which caused higher-order components to contaminate lower-order kernels in finite-length Volterra series.

Contamination of the linear impulse response by higher-order components in the Volterra series could potentially account for the differences in the WT and *Sh*^{14} kernels between naturalistic and white noise stimuli. To eliminate this possibility, we compared first-order kernels obtained by terminating the Volterra series at $K_1(u)$ or $K_3(u, v, w)$ (Fig. 3*C*). The kernel forms were similar: *Sh*^{14} first-order kernels obtained from third-order series still had larger amplitudes and faster time-to-peaks than those of WT kernels. However, the first-order kernels obtained from third-order series were significantly larger than those obtained by terminating the Volterra series at $K_1(u)$, indicating strongly nonlinear behavior, and that the second- and/or third-order kernels contain components of similar time course, but negative amplitude (Fig. 3*C*).

Previous analysis of WT and *Sh*^{14} voltage responses to white noise stimuli revealed negative amplitude nonlinearities on the diagonal of the second-order kernels, corresponding to a nonlinear attenuation (Juusola et al. 2003). Second-order kernels, $K_2(u, v)$, derived from naturalistic stimuli, did not contain these negative nonlinearities. Instead, they had positive peaks on the diagonals having approximately the same time courses as the first-order kernels (Fig. 3, *D* and *E*). This pattern of kernel forms is characteristic of the Hammerstein nonlinear model (Korenberg and Hunter 1986) in which a linear filter is followed by a static nonlinearity. However, the second-order kernels also had many nonzero values away from the diagonals, indicating that additional, complex nonlinear interactions were significant.

NLN cascade model of phototransduction

The pattern of kernel forms derived from the first- and second-order kernels of the Volterra series suggested that the WT and *Sh*^{14} photoreceptor responses could be described by a model in which a dynamic linear filter is followed by a static nonlinearity (French and Korenberg 1989; Korenberg and Hunter 1986). This model is attractive because it may potentially correspond to the phototransduction cascade (linear filter) and the photoinsensitive membrane (static nonlinearity) of the photoreceptor. Such a model would have relatively few parameters and could be used to separate the effects of individual components of phototransduction and the photoinsensitive membrane, allowing mechanistic insights into the generation of the photoreceptor voltage responses (van Hateren and Snippe 2001). We tested several LN, NL, and NLN models to determine which model gave the best prediction of photoreceptors responses to naturalistic stimuli. The most successful of these models was an NLN model with a "Wong and Knight" or gamma function model of phototransduction (Wong et al. 1980) as the linear dynamic component surrounded by 2 static nonlinearities (Figs. 2 and 4). The first nonlinearity required a fifth-order polynomial, whereas the second polynomial was third-order, giving a total count of 10 parameters (see METHODS and Fig. 4). The NLN model captured a large part of the nonlinear photoreceptor behavior identified by the Volterra series (Fig. 2; Table 1).

Sh^{14} photoreceptors differed most strongly from WT photoreceptors in the second and third stages of the NLN model (Fig. 4, Table 2). The first static nonlinearity was a positive rectification, in which the response increased strongly above about 6.0 contrast units. This effect was slightly stronger in *Sh*^{14} flies. Linear components were very similar to first-order Volterra kernels, and the mutant flies again showed larger and faster responses, peaking about 2 ms before the WT. The final static nonlinearity always had a region of zero, or negative slope in the middle of an overall positive characteristic, corresponding to an intermediate region where increasing light intensity produced no change, or a slight hyperpolarization, in membrane potential. In *Sh*^{14} photoreceptors this effect occurred over a

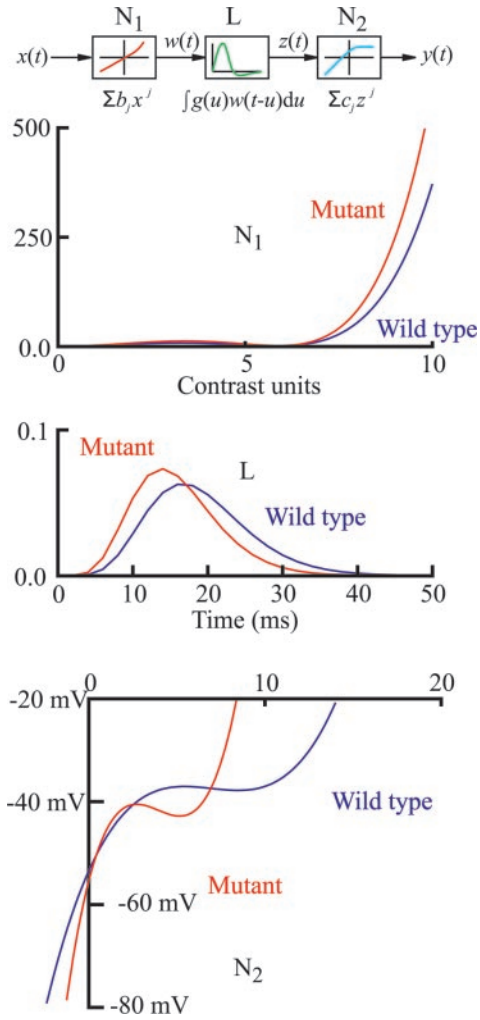

FIG. 4. NLN cascade model of phototransduction. Input light contrast signal $x(t)$ was assumed to pass through a static nonlinearity N_1, to a linear, time-dependent filter L, leading to a final static nonlinearity N_2. Intermediate signals were $w(t)$ and $z(t)$, and the final output signal was $y(t)$. Static nonlinearities were modeled by fifth- and third-order polynomial functions, respectively. Linear filter was the Wong and Knight function of *Eq. 2*. Fitted components of the NLN model are shown for typical WT and *Sh*^{14} mutant *Drosophila* photoreceptors (Table 2). *Top*: first static nonlinearity was strongly rectifying at high contrasts, slightly stronger in mutants. *Middle*: linear filters closely resembled the first-order Volterra kernels. *Bottom*: second static nonlinearity always showed a region of zero or negative slope, with mutant receptors passing through this region at lower contrast levels. Because linear amplification or attenuation can occur at any stage of a cascade, the only parameters with absolute significance are the dimensionless contrast input values along the abscissa of the *top graph*, and the membrane potential output along the ordinate of the *bottom graph*.

TABLE 2. *Fitted parameters of NLN cascade models of experimental data*

First Nonlinear				Linear			Second Nonlinear		
c_2	c_3	c_4	c_5	n	τ, ms	Offset	c_1, mV	c_2, mV	c_3, mV
				Wild-type					
1.072	0.230	−0.179	0.018	7.081	2.354	0.022	7.658	−1.156	0.055
0.947	0.247	−0.152	0.014	7.172	2.438	0.012	7.639	−1.175	0.060
1.034	0.172	−0.165	0.017	7.192	2.473	0.044	8.062	−0.951	0.034
1.358	0.338	−0.241	0.024	7.323	2.531	0.025	8.008	−0.979	0.037
1.979	0.618	−0.379	0.036	6.587	2.055	0.003	7.578	−1.236	0.062
				Sh^{14}					
1.365	0.275	−0.225	0.023	6.645	2.097	0.004	13.201	−3.765	0.326
1.570	0.399	−0.282	0.028	6.584	2.036	0.003	13.922	−3.399	0.254
1.602	0.419	−0.292	0.029	6.662	2.082	0.003	13.870	−3.423	0.256
1.573	0.387	−0.279	0.028	6.491	1.978	0.001	13.256	−3.727	0.316
1.380	0.361	−0.248	0.025	6.699	2.129	0.000	13.311	−3.695	0.323

Input signal was in dimensionless contrast units. Conversion to output in mV was assumed to occur in the second polynomial function. Parameter $c_1 = 1$ for the first polynomial function (see METHODS).

smaller stimulus range and at lower stimulus levels, corresponding to less depolarized membrane potentials.

Do differences in the light-induced current between Sh^{14} and WT photoreceptors contribute to differences in their voltage responses to naturalistic stimuli?

Although some of differences in the voltage responses of WT and Sh^{14} photoreceptors can be attributed directly to the *Shaker* channel (see DISCUSSION), it is also possible that changes in the LIC or other ionic currents could occur during development. We used a Hodgkin–Huxley model of the *Drosophila* photoreceptor (Niven et al. 2003a,b) to determine whether these differences in LIC or voltage-gated ion channels contribute to the observed differences between WT and Sh^{14} responses. This model allowed us to separate the effects of the LIC and voltage-gated currents that contributed to voltage responses.

After recording responses of *Drosophila* photoreceptors to naturalistic and white noise light stimuli we injected current steps to characterize the photoreceptor membrane properties (see METHODS). These membrane properties were used to construct a Hodgkin–Huxley model of the photoinsensitive membrane of each WT or Sh^{14} photoreceptor (Niven et al. 2003a,b). We then used this model to estimate the LIC, delayed rectifier current, and, in WT photoreceptors, the *Shaker* current to the same NTSI stimulus (Fig. 5, *A*, *D*, and *F*). There were several differences between the currents in WT and Sh^{14} models (other than the absence of functional *Shaker* channels) including an increase in the LIC and the delayed rectifier current in Sh^{14} photoreceptor responses (Fig. 5, *C* and *G*). The structure of both the WT and Sh^{14} LICs resembled both the gross structure of the naturalistic light stimulus and the photoreceptor voltage responses. Examination of the fine structure of the LICs revealed that they were more similar than the equivalent voltage responses. In particular, the WT LIC showed the same compression of signals as the Sh^{14} LIC during sequences of rapid transients. However, during these sequences of light pulses the WT voltage response followed the light stimulus, whereas the Sh^{14} did not. Additionally, many of the transients visible in the

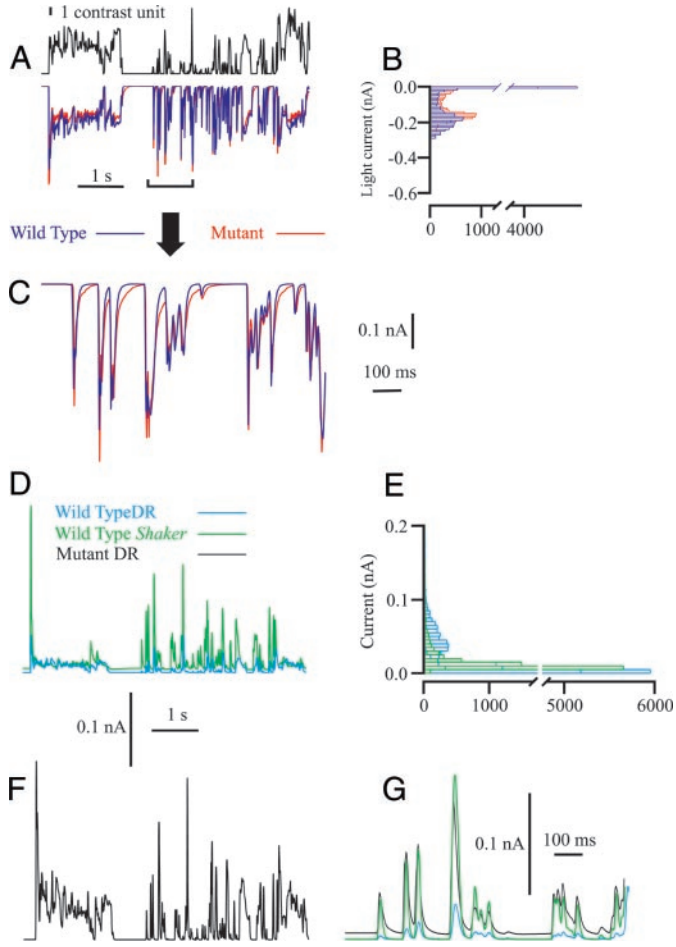

FIG. 5. Responses of Hodgkin–Huxley style numerical models of WT and Sh^{14} mutant *Drosophila* photoreceptors to naturalistic time series light stimuli (see METHODS). *A*: model light currents produced by the same contrast stimulus used in the photoreceptor recordings (see Fig. 1). *B*: *frequency histograms* for the entire records. *C*: portion of the *light current traces* shown on an expanded time scale. *D*: model WT delayed rectifier and *Shaker* currents during the same period of NTSI light stimulation. *E*: *frequency histograms* of WT delayed rectifier and *Shaker* currents for the entire record. *F*: model mutant delayed rectifier current under the same conditions. *G*: comparison of all 3 model potassium currents at higher temporal resolution.

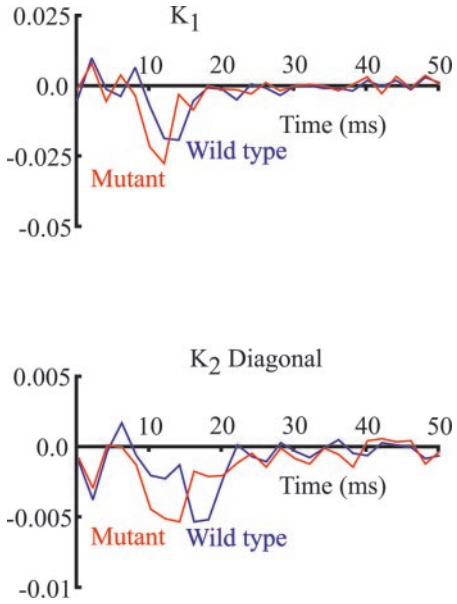

FIG. 6. First- and second-order kernels for the relationship between naturalistic time series light stimulation and light current in WT and mutant numerical models. Comparison with the experimental kernels (Fig. 3) indicates that the time course of the light current dominates the overall photoreceptor response.

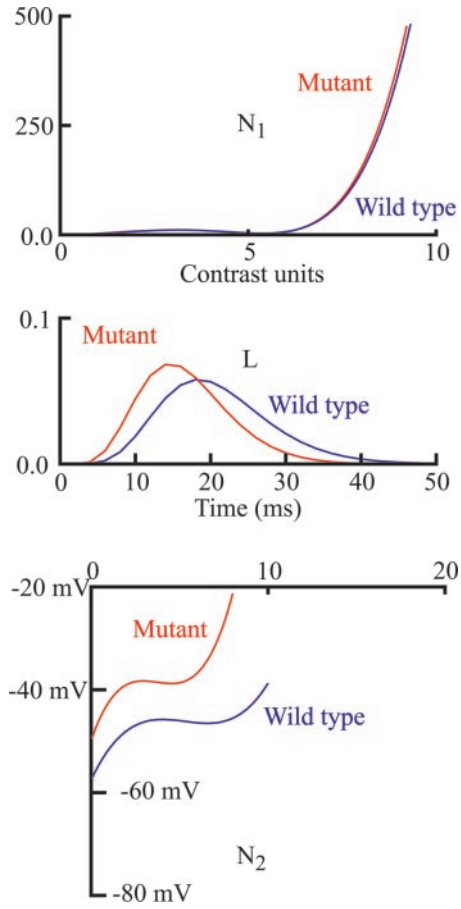

FIG. 7. NLN models of voltage responses of the numerical models of *Drosophila* photoreceptors. Note the close similarity to Fig. 4, indicating good agreement between the experimental and simulated data. The NLN model suggests that, although the strongest nonlinearity is a rectification process occurring early in the phototransduction process, differences between WT and mutant animals appear first in the linear component, which resembles the light current response. Differences are also seen in the final nonlinearities, whose negative slope regions and voltage ranges suggest analogy with voltage-activated conductances.

Sh^{14} voltage response corresponded to small, high-frequency fluctuations in the LIC.

To compare the differences in the WT and Sh^{14} simulated LICs with the differences in their experimental voltage responses, we calculated Volterra kernels between the naturalistic light stimulus and the LIC (Fig. 6, Table 3) and derived NLN models of the simulated LIC (Fig. 7, Table 4). There were close similarities between the time courses of the first- and second-order Volterra kernels (Fig. 6) and those derived from the WT and Sh^{14} voltage responses (Fig. 3), suggesting that light current dominates the dynamic response. The NLN models of the simulated LIC (Fig. 7, Table 4) also closely resembled those from the experimental data. As with the NLN model of the photoreceptor voltage responses, the NLN model consisted of a Wong and Knight function surrounded by 2 static nonlinearities. The first nonlinearity was indistinguishable between WT and Sh^{14} photoreceptors and reproduced the strong rectification in the first nonlinearity of the NLN model of photoreceptor voltage responses. The Wong and Knight function had a faster time-to-peak in the Sh^{14} LIC than in WT, which was similar to the differences between this component in the NLN model of WT and Sh^{14} voltage responses (Fig. 7). The main difference between the NLN model of the LIC and that of the voltage responses was in the second nonlinearity. This component was similar for both WT and Sh^{14} LICs (Fig. 7), unlike the same component for the voltage responses in which the WT had much larger negative slope regions at higher voltages (Fig. 4). Therefore although some of the differences between WT and Sh^{14} photoreceptors are directly attributed to loss of *Shaker* channels, there are also differences in the LIC (see DISCUSSION).

TABLE 3. *MSE values for Volterra kernel and NLN models of Hodgkin–Huxley currents*

Photoreceptor	K_1	K_2	NLN
Wild-type			
Light current	14.4	7.5	13.9
Delayed rectifier current	18.7	8.0	
Shaker current	67.2	28.7	
Sh^{14}			
Light current	18.8	5.6	10.9
Delayed rectifier current	25.3	12.2	

Values are expressed as percentage.

Changes in the delayed rectifier current in Sh^{14} photoreceptors

Comparison of the delayed rectifier currents from WT and Sh^{14} voltage responses simulated by the Hodgkin–Huxley model revealed that in the absence of the *Shaker* current there was a marked increase in the delayed rectifier current (Fig. 5, *D–G*). Additionally, WT delayed rectifier was slower than Sh^{14} delayed rectifier (Fig. 5*G*). What contribution do these changes in delayed rectifier current have on naturalistic stimulus processing? We calculated first-order Volterra kernels between the NTSI stimulus and the voltage-gated currents of the Hodgkin–Huxley simulations (Fig. 8, Table 3). These kernels had time

TABLE 4. *Fitted parameters of NLN cascade models of Hodgkin–Huxley light current*

First Nonlinear				Linear			Second Nonlinear		
c_2	c_3	c_4	c_5	n	τ, ms	Offset	c_1, mV	c_2, mV	c_3, mV
Wild-type									
1.237	0.279	−0.213	0.022	6.505	1.983	0.003	−0.104	0.030	−0.003
Sh^{14}									
1.151	0.354	−0.208	0.020	6.175	1.767	0.000	−0.094	0.023	−0.002

courses similar to those of the LICs but started ≤5 ms later. In the WT photoreceptors the kernel of the *Shaker* current was much larger than that of the delayed rectifier. However, the amplitude of the delayed rectifier kernels in the mutant were increased in comparison to those of the WT and reflected the partial replacement of *Shaker* by delayed rectifier current in the mutant model. We also calculated second-order Volterra kernels to ensure that the increase in the first-order mutant delayed rectifier kernel was not the consequence of contamination by higher-order kernels. The most prominent feature of all the second-order kernels in both WT and Sh^{14} photoreceptors was a relatively flat valley extending about 5 ms on either side of the diagonal (Fig. 8). This time corresponds approximately to the initial delay in the rise of the light current (Figs. 6 and 7).

DISCUSSION

Much neuronal activity is controlled by the specific properties of voltage-gated potassium channels (e.g., Connor and Stevens 1971; Weckström et al. 1991), but the roles of these channels in shaping neuronal responses during natural stimuli remain largely unknown. We addressed this problem by comparing in vivo recordings and nonlinear models of WT and Sh^{14} *Drosophila* photoreceptors coding naturalistic stimuli. Voltage responses of Sh^{14} photoreceptors to naturalistic stimuli were altered compared with their WT counterparts. In particular, many of the transient responses to naturalistic stimuli in Sh^{14} photoreceptors were distorted, and the spread of the signal over the available voltage range was reduced in Sh^{14} photoreceptors (Fig. 1). Modeling the responses of both photoreceptor types as Volterra kernels or NLN cascades suggested that these differences were attributable to larger, faster and shorter responses in Sh^{14} photoreceptors (Figs. 3 and 4). Models obtained from naturalistic stimuli were not the same as those from white noise stimuli (Juusola et al. 2003; Niven et al. 2003a), and differences between Sh^{14} and WT photoreceptors could not be predicted from the white noise models, suggesting that *Shaker* channels behave differently under different stimulus regimes (Fig. 3). To test whether these differences were attributed to conductance changes in the photoinsensitive membrane or to changes in the current through light-dependent channels (LIC), we used a Hodgkin–Huxley simulation of *Drosophila* photoreceptors to calculate the LIC of both WT and Sh^{14} photoreceptors. Simulated LICs of the WT and Sh^{14} photoreceptors were more similar than their voltage responses, suggesting a significant contribution of *Shaker* channels to encoding of naturalistic stimuli (Fig. 5). However, the simulations indicated that differences between WT and mutant photoreceptors were not restricted to *Shaker* potassium channels, but included changes in both LIC and delayed rectifier channels.

What causes the differences between photoreceptor responses to naturalistic and white noise stimuli?

WT photoreceptors had smaller-amplitude, longer time-to-peak, and longer half-width linear impulse responses than those of Sh^{14} mutants, which was also true for the linear component of the NLN model (Figs. 3 and 4). These differences between WT and Sh^{14} photoreceptor linear impulse responses may be explained, at least partially, by the presence or absence of functional *Shaker* K^+ channels in the photoinsensitive membrane of the photoreceptors. Increasing light intensity depolarizes WT photoreceptors, rapidly activates *Shaker* K^+ channels, and partially shunts the LIC through the increased membrane conductance (Niven et al. 2003a). The *Shaker* K^+ channels then rapidly inactivate, which effectively amplifies the effect of the LIC at later times in the photoreceptor voltage response. Thus WT photoreceptor impulse responses are expected to have longer time-to-peak, smaller amplitude, and longer half-width compared with Sh^{14} impulse responses.

In contrast, we previously showed that WT and Sh^{14} photoreceptor linear kernels have similar time-to-peak, amplitude, and half-width when measured with white noise stimulation (Fig. 3*B*). Under these conditions, differences between WT and Sh^{14} photoreceptors can be seen in the second-order kernel, where WT photoreceptors show an early nonlinear amplification that is absent in the Sh^{14} mutants (Juusola et al. 2003). Differences between kernels derived from naturalistic and white noise stimuli are attributed to the stimulus structure. Naturalistic stimuli can contain prolonged dark periods interspersed with periods of high light intensity, evoking large fluctuations in photoreceptor voltage (van Hateren 1997), whereas dark and bright periods in band-limited Gaussian white noise stimuli of similar duration are typically brief, allowing photoreceptor responses to be modulated around a relatively constant mean voltage. *Shaker* K^+ channels behave differently under these 2 stimulation regimes because their prominent activation and inactivation during voltage transients are reduced by maintained depolarization.

Can the differences between the WT and Sh^{14} photoreceptor responses to naturalistic stimuli be explained fully by the presence or absence of functional Shaker K^+ channels in the photoinsensitive membrane?

In vivo intracellular recordings of Sh^{14} photoreceptors suggest that they have a reduced input resistance to compensate for their lack of functional *Shaker* K^+ channels, which is accompanied by a depolarized resting potential (Niven et al. 2003a). However, it is also possible that the loss of *Shaker* K^+ channels

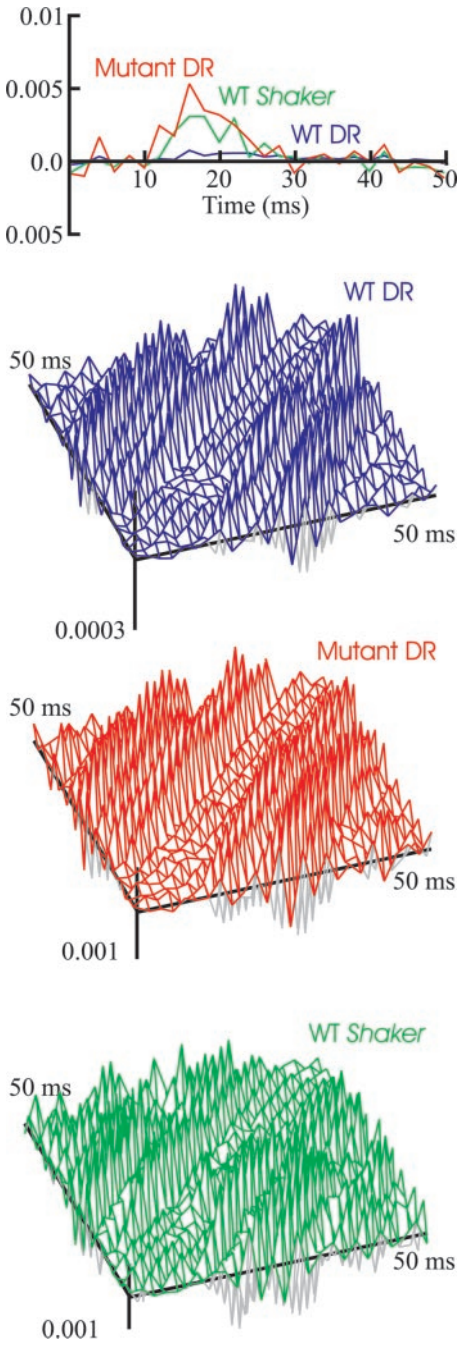

FIG. 8. First- and second-order kernels between light stimulation and potassium currents in WT and mutant numerical models of *Drosophila* phototransduction. Amplitudes of the kernels reflect the partial replacement of lost *Shaker* current by delayed rectifier current in the mutant model. Second-order kernels had generally diagonal structures, reflecting the strong initial nonlinearities of the NLN models. However, another major feature of the second-order kernels was a relatively flat valley about 10 ms wide along the diagonal, suggesting that nonlinear interactions with relative time displacements >5 ms dominate the nonlinear behavior.

affects the current flowing through light-dependent channels (LIC) through one or more feedback mechanisms. Such feedback could occur directly by changes in the voltage driving the LIC caused by changes in the numbers of different channel types in the photoinsensitive membrane. Alternatively, changes in channel populations could, through changes in membrane potential or ionic concentrations, modify the development of the components that generate the LIC. Both these possibilities must be considered.

Comparison of LIC kernels calculated from WT and Sh^{14} photoreceptors showed that mutant kernels were larger and faster than those of WT. Similarly, the linear Wong and Knight component of the NLN model, which may represent LIC generation, had a faster time-to-peak in mutant photoreceptors. These differences in the LIC cannot be ascribed directly to the presence or absence of *Shaker* K^+ channels because Sh^{14} photoreceptors are depolarized at rest relative to WT photoreceptors (Niven et al. 2003a), effectively reducing the driving force on the LIC (Reuss et al. 1997). This suggests that differences in the light-transduction machinery of the 2 phenotypes are caused by feedback that is not simply a change in driving potential.

What changes in light transduction might be expected? In *Drosophila* photoreceptors (Wu and Pak 1975), as in other photoreceptors (Baylor et al. 1979; Yeandle 1985), discrete electrical events (bumps) can be recorded under dim illumination that correspond to single-photon absorptions. Although the LIC predicted by simulation is faster in Sh^{14} photoreceptors, in vitro recordings show that bump amplitude, quantum efficiency, and macroscopic kinetics are unaffected (Niven et al. 2003a). Therefore differences between the phototransduction cascade of WT and Sh^{14} photoreceptors are unlikely to be the result of differences in bump amplitude and waveform. However, individual bumps are responses to single photons, whereas the Volterra kernels and NLN model in our analysis were calculated from responses to approximately 10^6 photons/s or more (Juusola and Hardie 2001). As mean light intensity increases, the average bump size decreases markedly and the time course is reduced (Juusola and Hardie 2001; Wu and Pak 1978). These changes in bump waveform may be the result of Ca^{2+}-mediated adaptation (Henderson et al. 2000), which is a feature of many invertebrate and vertebrate photoreceptors (Burns and Baylor 2001; Fain et al. 2001; Hardie and Minke 1995; Montell 1999; Pugh et al. 1999). Changes in light and dark adaptation mediated by Ca^{2+} have been proposed to explain differences between photoreceptor responses within an individual compound eye (Burton et al. 2001). One possibility is that Sh^{14} photoreceptors possess altered Ca^{2+} dynamics compared with WT, affecting light adaptation and the dynamics of the linear impulse response. An alternative explanation is that there are different distributions of bump latencies, such as would arise from shifting transduction to different regions of the photosensitive membrane.

The relative success of the NLN model suggests a functional analogy, in which the linear Wong and Knight component represents LIC generation. In this case, the 2 nonlinearities would occur before and after phototransduction, and could represent an early adaptation mechanism and the photoinsensitive membrane, respectively. Association of the final nonlinearity with the photoinsensitive membrane is supported by comparison of WT and Sh^{14} NLN models for the LIC with those of the voltage response. The final nonlinearity contains significant differences in the NLN models of the voltage response that are absent in the NLN models of the LIC. This suggests that the final nonlinearity is most affected by the properties of the photoinsensitive membrane. The first nonlinear component of the NLN models of LIC is similar for both WT and Sh^{14} photoreceptors, suggesting that this component

cannot account for the differences in the LIC. However, the linear component is faster in Sh^{14} photoreceptors, supporting the idea that differences in LIC are attributed to differences in the light transduction machinery.

Interaction between Shaker and delayed rectifier K^+ channels during naturalistic stimuli

The biophysical properties of *Shaker* and delayed rectifier channels are well characterized in *Drosophila* photoreceptors (Hardie 1991; Hardie et al. 1991). In WT photoreceptors *Shaker* channels are activated at the onset of a light impulse but inactivate rapidly, whereas delayed rectifier channels activate/inactivate more slowly (Niven et al. 2003a). The delayed rectifier current is larger in Sh^{14} than in WT photoreceptors (Fig. 5) because of interactions between delayed rectifier and *Shaker* channels. *Shaker* channels effectively shunt photoreceptor currents, not only reducing the overall size of delayed rectifier current but also changing the time course of activation (Niven et al. 2003a). These changes lead to a significantly smaller and slower first-order kernel for the WT delayed rectifier current compared with Sh^{14} (Fig. 8).

Functional significance

The change in LIC observed in Sh^{14} photoreceptors extends previous findings that activity of the phototransduction cascade may alter photoreceptor membrane properties (Burton 2002; Wolfram et al. 2003) by showing that these interactions may be bidirectional. Enabling photoreceptors to adjust photoinsensitive membrane properties to their LIC may ensure that photoreceptor voltage response is optimized to the prevailing light conditions. Changes in the LIC suggest that activity-dependent plasticity in *Drosophila* photoreceptors may occur by a feedback mechanism that is sensitive to changes in the photoreceptor membrane.

Alterations of the photoreceptor membrane, phototransduction cascade, or both represent tuning of these components to the lighting conditions experienced by the photoreceptor during development and adult life. Photoreceptor membrane properties are also thought to be tuned during evolution to the visual ecology of the insect by voltage-gated K^+ and Na^+ channels (for review see Weckström and Laughlin 1995). Our results suggest that individual ion channels, such as the *Shaker* K^+ channel, may filter the LIC in different ways depending on the dynamic properties of the stimulus. Therefore to understand the precise contribution of these channels to the voltage response of a neuron it is important to assess the properties of channels under the most natural possible stimulus conditions.

ACKNOWLEDGMENTS

We thank S. Laughlin and M. Weckström for comments and suggestions on the manuscript.

Present address of J. Niven: Department of Zoology, University of Cambridge, Cambridge CB2 1TN, UK.

GRANTS

This work was supported by grants from the Canadian Institutes of Health Research to A. S. French, and the Royal Society, Wellcome Trust, and Biotechnology and Biological Sciences Research Council to M. Juusola.

REFERENCES

Baylor DA, Lamb TD, and Yau KW. Responses of retinal rods to single photons. *J Physiol* 288: 613–634, 1979.

Burns ME and Baylor DA. Activation, deactivation, and adaptation in vertebrate photoreceptor cells. *Annu Rev Neurosci* 24: 779–805, 2001.

Burton BG. Long-term light adaptation in photoreceptors of the housefly, *Musca domestica*. *J Comp Physiol A Sens Neural Behav Physiol* 188: 527–538, 2002.

Burton BG and Laughlin SB. Neural images of pursuit targets in the photoreceptor arrays of male and female houseflies *Musca domestica*. *J Exp Biol* 15: 3963–3977, 2003.

Burton BG, Tatler BW, and Laughlin SB. Variations in photoreceptor response dynamics across the fly retina. *J Neurophysiol* 86: 950–960, 2001.

Burton GJ and Moorhead IR. Visual form perception and the spatial phase transfer function. *J Opt Soc Am* 71: 1056–1063, 1981.

Chacron MJ, Doiron B, Maler L, Longtin A, and Bastian J. Non-classical receptive field mediates switch in a sensory neuron's frequency tuning. *Nature* 423: 77–81, 2003.

Connor JA and Stevens CF. Voltage clamp studies of a transient outward membrane current in gastropod neural somata. *J Physiol* 213: 21–30, 1971.

Dan Y, Atick JJ, and Reid RC. Efficient coding of natural scenes in the lateral geniculate nucleus: experimental test of a computational theory. *J Neurosci* 16: 3351–3362, 1996.

David CT. The relationship between body angle and flight speed in free-flying *Drosophila*. *Physiol Ent* 3: 191–195, 1978.

Fain GL, Matthews HR, Cornwall MC, and Koutalos Y. Adaptation in vertebrate photoreceptors. *Physiol Rev* 81: 117–151, 2001.

Field DJ. Relations between the statistics of natural images and the response properties of cortical cells. *J Opt Soc Am A* 4: 2379–2394, 1987.

French AS. Phototransduction in the fly compound eye exhibits temporal resonances and a pure time delay. *Nature* 283: 200–202, 1980.

French AS and Korenberg MJ. A nonlinear cascade model for action potential encoding in an insect sensory neuron. *Biophys J* 55: 655–661, 1989.

French AS, Korenberg MJ, Järvilehto M, Kouvalainen E, Juusola M, and Weckström M. The dynamic nonlinear behavior of fly photoreceptors evoked by a wide range of light intensities. *Biophys J* 65: 832–839, 1993.

French AS and Marmarelis VZ. Nonlinear analysis of neuronal systems. In: *Modern Techniques in Neuroscience Research*, edited by Windhorst U and Johansson H. Berlin: Springer-Verlag, 1999, p. 627–640.

French AS, Sekizawa S, Höger U, and Torkkeli PH. Predicting the responses of mechanoreceptor neurons to physiological inputs by nonlinear system identification. *Ann Biomed Eng* 29: 187–194, 2001.

Fry SN, Sayaman R, and Dickinson MH. The aerodynamics of free flight maneuvers in *Drosophila*. *Science* 300: 495–498, 2003.

Gerster U. A quantitative estimate of flash-induced Ca(2+)- and Na(+)-influx and Na^+/Ca(2+)-exchange in blowfly *Calliphora* photoreceptors. *Vision Res* 37: 2477–2485, 1997.

Gerster U, Stavenga DG, and Backhaus W. Na^+/K^+-pump activity in photoreceptors of the blowfly *Calliphora*: a model analysis based on membrane potential measurements. *J Comp Physiol A Sens Neural Behav Physiol* 180: 113–122, 1997.

Hardie RC. Voltage-sensitive potassium channels in *Drosophila* photoreceptors. *J Neurosci* 11: 3079–3095, 1991.

Hardie RC and Minke B. Phosphoinositide-mediated phototransduction in *Drosophila* photoreceptors: the role of Ca^{2+} and TRP. *Cell Calcium* 18: 256–274, 1995.

Hardie RC, Voss D, Pongs O, and Laughlin SB. Novel potassium channels encoded by the *Shaker* locus in *Drosophila* photoreceptors. *Neuron* 6: 477–486, 1991.

Henderson SR, Reuss H, and Hardie RC. Single photon responses in *Drosophila* photoreceptors and their regulation by Ca^{2+}. *J Physiol* 524: 179–194, 2000.

Hevers W and Hardie RC. Serotonin modulates the voltage dependence of delayed rectifier and *Shaker* potassium channels in *Drosophila* photoreceptors. *Neuron* 14: 845–856, 1995.

Juusola M and de Polavieja GG. The rate of information transfer of naturalistic stimulation by graded potentials. *J Gen Physiol* 122: 191–206, 2003.

Juusola M and Hardie RC. Light adaptation in *Drosophila* photoreceptors. I. Response dynamics and signaling efficiency at 25 degrees C. *J Gen Physiol* 117: 3–25, 2001.

Juusola M, Kouvalainen E, Järvilehto M, and Weckström M. Contrast gain, signal-to-noise ratio, and linearity in light-adapted blowfly photoreceptors. *J Gen Physiol* 104: 593–621, 1994.

Juusola M, Niven JE, and French AS. *Shaker* K^+ channels contribute early nonlinear amplification to the light response in *Drosophila* photoreceptors. *J Neurophysiol* 90: 2014–2021, 2003.

Kaplan WD and Trout WE. The behavior of four neurological mutants of *Drosophila*. *Genetics* 61: 399–409, 1961.
Katz LC and Shatz CJ. Synaptic activity and the construction of cortical circuits. *Science* 274: 1133–1138, 1996.
Korenberg MJ. Parallel cascade identification and kernel estimation for nonlinear systems. *Ann Biomed Eng* 19: 429–455, 1991.
Korenberg MJ and Hunter IW. The identification of nonlinear biological systems: LNL cascade models. *Biol Cybern* 55: 125–134, 1986.
Laughlin SB and Hardie RC. Common strategies for light adaptation in the peripheral visual systems of fly and dragonfly. *J Comp Physiol* 128: 319–340, 1978.
Lewen GD, Bialek W, and de Ruyter van Steveninck RR. Neural coding of naturalistic motion stimuli. *Network* 12: 317–329, 2001.
Marmarelis PZ and Marmarelis VZ. *Analysis of Physiological Systems*: *The White-Noise Approach.* New York: Plenum Press, 1978.
Montell C. Visual transduction in *Drosophila*. *Annu Rev Cell Dev Biol* 15: 231–268, 1999.
Niven JE and Burrows M. Spike width reduction modifies the dynamics of short-term depression at a central synapse in the locust. *J Neurosci* 23: 7461–7469, 2003.
Niven JE, Vähäsöyrinki M, and Juusola M. *Shaker* K(+)-channels are predicted to reduce the metabolic cost of neural information in *Drosophila* photoreceptors. *Proc R Soc Lond B Biol Sci* 270, *Suppl.* 1: S58–S61, 2003.
Niven JE, Vähäsöyrinki M, Kauranen M, Hardie RC, Juusola M, and Weckström M. The contribution of *Shaker* K(+) channels to the information capacity of *Drosophila* photoreceptors. *Nature* 421: 630–634, 2003.
Oberwinkler J and Stavenga DG. Calcium transients in the rhabdomeres of dark- and light-adapted fly photoreceptor cells. *J Neurosci* 20: 1701–1709, 2000.
Press WH, Flannery BP, Teukolsky SA, and Vetterling WT. *Numerical Recipes in C. The Art of Scientific Computing.* Cambridge, UK: Cambridge Univ. Press, 1990.
Pugh EN Jr, Nikonov S, and Lamb TD. Molecular mechanisms of vertebrate photoreceptor light adaptation. *Curr Opin Neurobiol* 9: 410–418, 1999.
Reinagel P. How do visual neurons respond in the real world? *Curr Opin Neurobiol* 11: 437–442, 2001.
Reuss H, Mojet MH, Chyb S, and Hardie RC. *In vivo* analysis of the *Drosophila* light-sensitive channels, TRP and TRPL. *Neuron* 19: 1249–1259, 1997.
Rieke F, Bodnar DA, and Bialek W. Naturalistic stimuli increase the rate and efficiency of information transmission by primary auditory afferents. *Proc R Soc Lond B Biol Sci* 262: 259–265, 1995.
Rinberg D and Davidowitz H. A stimulus generating system for studying wind sensation in the American cockroach. *J Neurosci Methods* 121: 1–11, 2002.
Ruderman DL and Bialek W. Statistics of natural images: scaling in the woods. *Phys Rev Lett* 73: 814–817, 1994.
Salkoff L and Wyman R. Genetic modification of potassium channels in *Drosophila Shaker* mutants. *Nature* 293: 228–230, 1981.
Srinivasan MV, Laughlin SB, and Dubs A. Predictive coding: a fresh view of inhibition in the retina. *Proc R Soc Lond B Biol Sci* 216: 427–459, 1982.
Tolhurst DJ, Tadmor Y, and Chao T. Amplitude spectra of natural images. *Ophthalmic Physiol Opt* 12: 229–232, 1992.
van Hateren JH. Electrical coupling of neuro-ommatidial photoreceptor cells in the blowfly. *J Comp Physiol A Sens Neural Behav Physiol* 158: 795–811, 1986.
van Hateren JH. Processing of natural time series of intensities by the visual system of the blowfly. *Vision Res* 37: 3407–3416, 1997.
van Hateren JH and Snippe HP. Information theoretical evaluation of parametric models of gain control in blowfly photoreceptor cells. *Vision Res* 41: 1851–1865, 2001.
Vickers NJ, Christensen TA, Baker TC, and Hildebrand JG. Odour-plume dynamics influence the brain's olfactory code. *Nature* 410: 466–470, 2001.
Vinje WE and Gallant JL. Sparse coding and decorrelation in primary visual cortex during natural vision. *Science* 287: 1273–1276, 2000.
Vinje WE and Gallant JL. Natural stimulation of the nonclassical receptive field increases information transmission efficiency in V1. *J Neurosci* 22: 2904–2915, 2002.
Weckström M, Hardie RC, and Laughlin SB. Voltage-activated potassium channels in blowfly photoreceptors and their role in light adaptation. *J Physiol* 440: 635–657, 1991.
Weckström M and Laughlin SB. Visual ecology and voltage-gated ion channels in insect photoreceptors. *Trends Neurosci* 18: 17–21, 1995.
Wolfram V, Niven JE, and Juusola M. Experience-dependent plasticity, gain control and information capacity in Drosophila photoreceptors. *Proc 29th Göttingen Neurobiol Conf* Abstr. 529, 2003.
Wong F, Knight BW, and Dodge FA. Dispersion of latencies in photoreceptors of Limulus and the adapting bump model. *J Gen Physiol* 76: 517–537, 1980.
Wu CF and Pak WL. Quantal basis of photoreceptor spectral sensitivity of *Drosophila* melanogaster. *J Gen Physiol* 66: 149–168, 1975.
Wu CF and Pak WL. Light-induced voltage noise in the photoreceptor of *Drosophila melanogaster*. *J Gen Physiol* 71: 249–268, 1978.
Yeandle S. Statistics and quantum bumps in arthropod photoreceptors. *Fed Proc* 44: 2947–2949, 1985.
Zettler F. Die Abhangigkeit des Übertragungsverhaltens von Frequenz und Adaptionszustand; gemessen am einzelnen Lichtrezeptor von *Calliphora erythrocephala*. *Z Vergl Physiol* 64: 432–449, 1969.